AIP Advances

Topography evolution of germanium thin films synthesized by pulsed laser deposition

Cite as: AIP Advances **7**, 045115 (2017); https://doi.org/10.1063/1.4981800
Submitted: 01 February 2017 • Accepted: 09 April 2017 • Published Online: 17 April 2017

P. Schumacher, S. G. Mayr and B. Rauschenbach

View Online
Export Citation
CrossMark

ARTICLES YOU MAY BE INTERESTED IN

Review Article: Stress in thin films and coatings: Current status, challenges, and prospects
Journal of Vacuum Science & Technology A **36**, 020801 (2018); https://doi.org/10.1116/1.5011790

Role of hydrogen carrier gas on the growth of few layer hexagonal boron nitrides by metal-organic chemical vapor deposition
AIP Advances **7**, 045116 (2017); https://doi.org/10.1063/1.4982029

Ge(001) surface cleaning methods for device integration
Applied Physics Reviews **4**, 021308 (2017); https://doi.org/10.1063/1.4984975

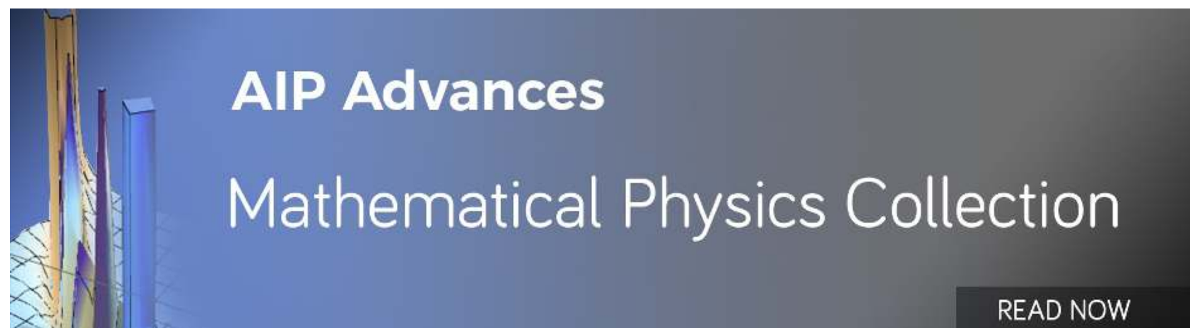

© 2017 Author(s).

AIP ADVANCES **7**, 045115 (2017)

Topography evolution of germanium thin films synthesized by pulsed laser deposition

P. Schumacher,[1,a] S. G. Mayr,[1,2] and B. Rauschenbach[1,2]
[1]*Leibniz-Instiut für Oberflächenmodifizierung (IOM), Permoserstr. 15, 04318 Leipzig, Germany*
[2]*Fakultät für Physik und Geowissenschaften, Universität Leipzig, 04103 Leipzig, Germany*

(Received 1 February 2017; accepted 9 April 2017; published online 17 April 2017)

Germanium thin films were deposited by Pulsed Laser Deposition (PLD) onto single crystal Ge (100) and Si (100) substrates with a native oxide film on the surface. The topography of the surface was investigated by Atomic Force Microscopy (AFM) to evaluate the scaling behavior of the surface roughness of amorphous and polycrystalline Ge films grown on substrates with different roughnesses. Roughness evolution was interpreted within the framework of stochastic rate equations for thin film growth. Here the Kardar-Parisi-Zhang equation was used to describe the smoothening process. Additionally, a roughening regime was observed in which 3-dimensional growth occurred. Diffusion of the deposited Ge adatoms controlled the growth of the amorphous Ge thin films. The growth of polycrystalline thin Ge films was dominated by diffusion processes only in the initial stage of the growth. © *2017 Author(s). All article content, except where otherwise noted, is licensed under a Creative Commons Attribution (CC BY) license (http://creativecommons.org/licenses/by/4.0/).* [http://dx.doi.org/10.1063/1.4981800]

I. INTRODUCTION

Since the first report of Pulsed Laser Deposition (PLD) in 1965,[1] it has become an established technique for coating surfaces and producing thin films. This technique has several advantages with respect to molecular beam epitaxy, among which are the high versatility, applicability and possibility to perform stoichiometric transfer, even with complicated compounds.[2,3] For applications of the PLD technique, it is important to understand the physical principles that govern the growth process. Recent studies performed with Ge have yielded results about the roughness evolution, parameter dependence of the epitaxial breakdown and coarsening of mound-like structures on the surface.[4–6] PLD has also been used to grow Ge nanostructures that have potential importance in device fabrication.[7]

This work contributes to the understanding of basic, physical mechanisms in thin film growth by PLD by taking into account the crystalline phase, film thickness, as well as substrate material for the growth of Ge as an exemplary material. Particularly, diffusion rates of adatoms in PLD can be increased and thereby change the surface topography significantly in comparison to other deposition techniques.[8] Consequently, the question arises, for which conditions diffusion processes dominate the growth. With this objective in mind, the scaling behavior of the surface roughness was investigated. By applying the power spectral density (PSD) function to the surface topography as obtained by an Atomic Force Microscope (AFM), physical mechanisms that govern the growth processes on certain length scales can be identified. The basic feasibility of such an approach has been demonstrated within different scopes previously.[9,10] In this context, the following continuum models that describe the surface evolution were considered. In a simplest case, random deposition is assumed, which means that particles are deposited on random positions and remain there. The growth exponent β, which characterizes the scaling behavior of the roughness over the time, can be calculated as β=0.5 for random deposition.[11] If surface diffusion is a dominant factor (in addition to random deposition)

[a]Electronic mail: philipp.schumacher@iom-leipzig.de

 © Author(s) 2017

the Wolf-Villain equation[12] that combines Mullins-Herring curvature-induced surface diffusion[13,14] with stochastic noise has been demonstrated to yield results in good accordance with experimental data:

$$\frac{\partial h(x,y,t)}{\partial t} = \text{-K}\,\nabla^4 h\,(x,y,t) + \eta(x,y,t). \tag{1}$$

Here, $h(x, y, t)$ is the height of the surface at position (x, y) for time t. K is a temperature dependent constant and $\eta(x, y, t)$ a noise term. For the first term, diffusion of particles on the surface is assumed to occur according to the local chemical potential, dependent on the local curvature of the surface. The second term is a noise term that takes into account the randomness of the process. For this process the growth exponent is β=0.25, assuming a two-dimensional system.[15] The roughness exponent α characterizes the scaling behavior of the roughness, depending on the length scale. For processes dominated by the Mullins-Herring equation, the roughness exponent is α=1 for two dimensions.[15] Another growth mechanism is represented by the Kardar-Parisi-Zhang equation[16]

$$\frac{\partial h(x,y,t)}{\partial t} = \nu\nabla^2 h\,(x,y,t) + \frac{\lambda}{2}\left[\nabla h(x,y,t)\right]^2 + \eta\,(x,y,t)\,, \tag{2}$$

where $h(x, y, t)$ is again the height of the surface at the position (x, y) and for time t. λ and ν are constants. The first term reflects a deposition-desorption phenomenon. Depending on the chemical potential of the vapor and surface, which depends on the local surface curvature, either desorption from or deposition onto the surface dominates. The second term reflects the existence of lateral growth, while the third term takes into account noise since random deposition is assumed. Growth which is governed by this equation shows a scaling behavior characterized by a roughness exponent α=0.39 and a growth exponent β=0.25.[17] These exponents are numerical results of the Kardar-Parisi-Zhang equation.

If three-dimensional growth occurs, the coarsening exponent γ describes the relationship between the film thickness and separation of mound-structures on the surface. For Ge films produced by PLD, Shin et al. experimentally found a coarsening exponent γ=0.40±0.05.[4]

II. EXPERIMENTAL CONDITIONS

In the present investigations, Ge films were deposited from a high purity Ge target by means of PLD. As substrates, Si (100) and Ge (100) were used. The native oxide layers on the substrates were not removed. A KrF-excimer laser with a pulse length of 20 ns and wavelength of 248 nm was used for PLD. The pulse frequency was 10 Hz and the pulse energy was fixed at 220 mJ, with a focal spot size of roughly 0.05 cm^2 that resulted in a fluence of 4.4 J/cm^2. For all depositions, the background pressure was $<8\times10^{-8}$ mbar. The average deposition rate was on the order of 0.001 nm per pulse. The thickness of the Ge films was controlled via the number of laser pulses and monitored by a quartz crystal microbalance, which was calibrated regularly by means of X-ray reflectometry. The substrates could be heated using a resistive heater and the temperature was corrected using a thermocouple. The topography of the films was investigated by an AFM in tapping mode with a scan size of 2x2 μm^2. The Si tips had a nominal radius of 7 nm. From the statistical point of view, the height fluctuations of the surface could be described by the root mean square roughness (RMS) R_q, which is given by

$$R_q = \sqrt{\frac{1}{NM}\sum\nolimits_{i=1}^{N}\sum\nolimits_{j=1}^{M}\left[h(x_i,y_j)-\bar{h}\right]^2}, \tag{3}$$

where $h(x_i, y_j)$ is the surface height at a given point (x_i, y_j), N and M are the number of points in x- and in y-direction, respectively and $\bar{h} = \frac{1}{NM}\sum_{i=1}^{N}\sum_{j=1}^{M} h(x_i, y_j)$ is the average height of the surface. The RMS value of each film was measured on a square area of 500 x 500 nm^2. During film growth, different points on the surface are not independent and the height at each point is related to the height at other points nearby. The information about these correlations and about characteristic distances of structures is provided by the height-height correlation function

$$H\left(\delta_x,\delta_y,t\right) = \left\langle \left[h\left(x+\delta_x, y+\delta_y, t\right) - h(x,y,t)\right]^2 \right\rangle, \tag{4}$$

where δ_x and δ_y are distances in x- and in y-direction respectively. The angular brackets denote averaging over the plane. Additionally, the PSD function was calculated in order to analyze the height profiles in reciprocal space. The scaling behavior of this function is related to the aforementioned roughness exponents.[18] It is therefore possible to deduce the physical principles governing the growth of the material. By performing the discrete two dimensional fast Fourier transformation (FFT) of the height profile of the AFM images, the dominating spatial frequencies on the surface and amplitude of the roughness can be determined. For the discrete case, a square image of N x N points, the two-dimensional fast Fourier transformation is given by

$$FFT\left(f_x, f_y\right) = \frac{1}{N^2} \sum_{i=1}^{N} \sum_{j=1}^{N} h\left(x_i, y_j\right) exp\left[-\frac{2i\pi}{N}\left(x_i f_x + y_j f_y\right)\right], \tag{5}$$

where f_x and f_y are the spatial frequency coordinates along the x-axis and y-axis, respectively. By calculation of the magnitude square of $FFT(f_x, f_y)$, the two-dimensional power spectral density function $PSD(f_x, f_y)$ can be obtained.[19] The structures on the surface were expected to be isotropic, so the angular averaged $PSD(f)$ was used to evaluate the experimental roughness data. The averaging was performed over all spatial frequencies with constant magnitude $f = \sqrt{f_x^2 + f_y^2}$. For the PSD function, an expression can be derived from which the contributing processes can be deduced[10]

$$PSD\left(f, t\right) = D(f)\frac{1 - e^{-2t\sum_{i=1}^{4} a_i f^i}}{\sum_{i=1}^{4} a_i f^i} \tag{6}$$

where $D(f)$ is the strength of the white noise, t is the time and $a_i \geq 0$ are constants whose relations contain information about the growth process and the dominating mechanisms.

III. RESULTS AND DISCUSSION

Epitaxial growth of Ge on Si (100) by physical vapor deposition has been previously observed (see e.g. Ref. 20). However, in this study, epitaxial growth was not expected due to the presence of native oxide on the substrates and the comparably low temperatures during the deposition process.

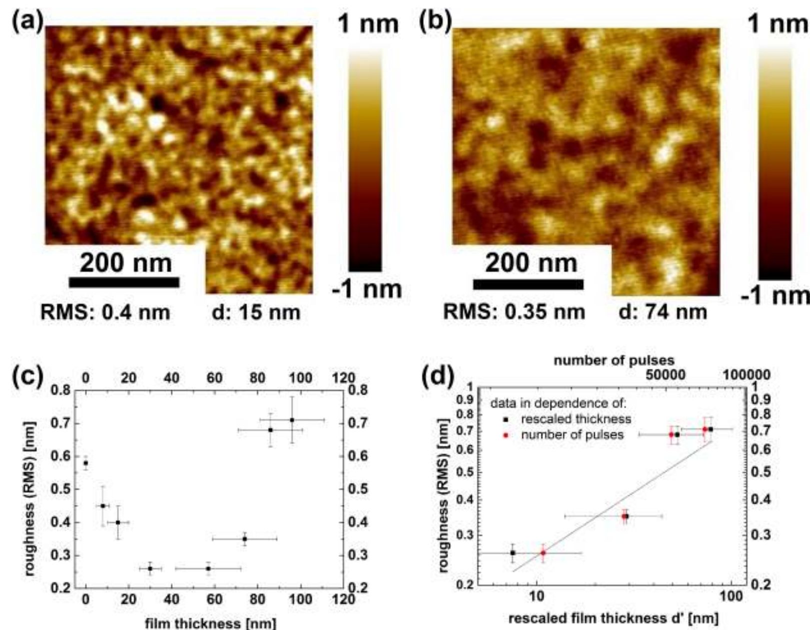

FIG. 1. (a,b) AFM images of polycrystalline Ge films deposited on Ge at 175 °C. The RMS value and the thickness d are given below each image. (c) The roughness evolution of polycrystalline Ge films deposited on Ge at 175 °C. (d) The evolution of the roughness in the roughening regime with a rescaled film thickness (see text), shown with a power law fit. The same data is also plotted with respect to the number of laser pulses, indicated by circular data points.

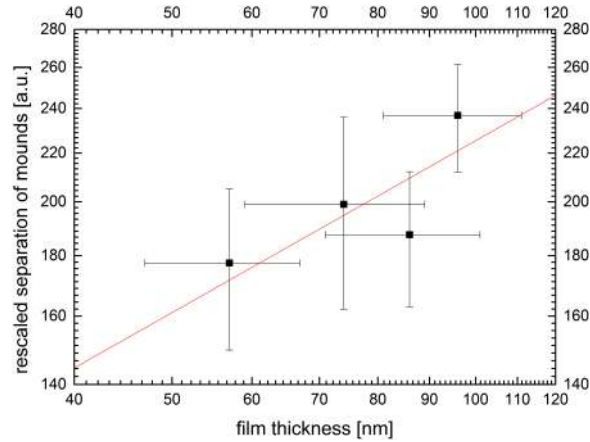

FIG. 2. The mound separation determined by the height-height correlation function with respect to the film thickness of polycrystalline Ge films deposited at 175 °C.

The evolution of the surface topography was studied by variation of both the substrate material and substrate temperature. The Ge deposition was either carried out at room temperature to produce amorphous films or at (175±30) °C to produce polycrystalline films.

In Figs. 1 (a) and (b), AFM images of polycrystalline Ge films deposited on Ge substrates and with two different film thicknesses are compared. Additionally, Fig. 1 presents the roughness evolution with respect to the film thickness. The AFM images and roughness evolution revealed that the deposited Ge film was not initially closed. The Ge film was smoothened until it closed above a critical layer thickness of approximately 45 nm. Consequently, the roughness rose with the layer thickness, which was caused by a coarsening process during the deposition. In agreement to the study of Shin et al.,[4] the formation of irregularly shaped mounds was observed. During the pulsed laser ablation process, the deposition rate was not constant; therefore, the film thickness was not a time-equivalent quantity. For this reason, the film thickness d was rescaled in order to determine the growth exponent. The rescaled and time-equivalent film thickness was calculated according to $d' = (\bar{r}/r)\,(d - 45nm)$. Here, d is divided by the time-averaged deposition rate r of each sample and multiplied by a constant $\bar{r}$. This rescaling generated the film thickness that would exist if all the samples were deposited at a constant deposition rate of $\bar{r}$. The result of this rescaling is depicted in Fig. 1 (d). The growth exponent β could be determined for the roughening regime above a film

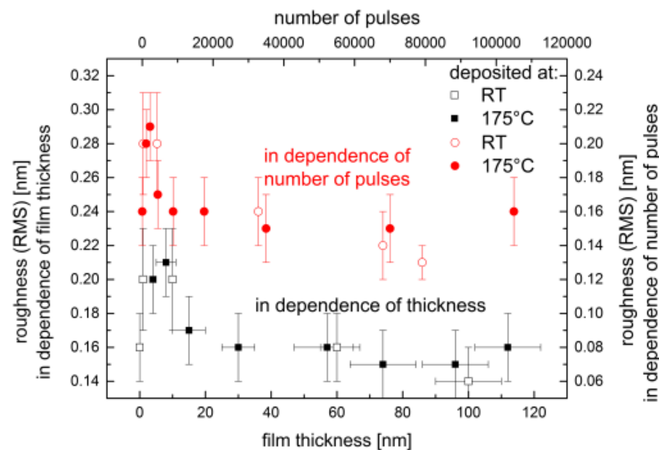

FIG. 3. The roughness evolution of Ge films on Si substrates at two different temperatures. The filled points represent the data for the polycrystalline films (deposited at 175 °C), while the hollow points represent the data for the amorphous films (deposited at room temperature). The circular points (red) show the roughness evolution with respect to the number of laser pulses, and the square points (black) show the roughness evolution with respect to the film thickness.

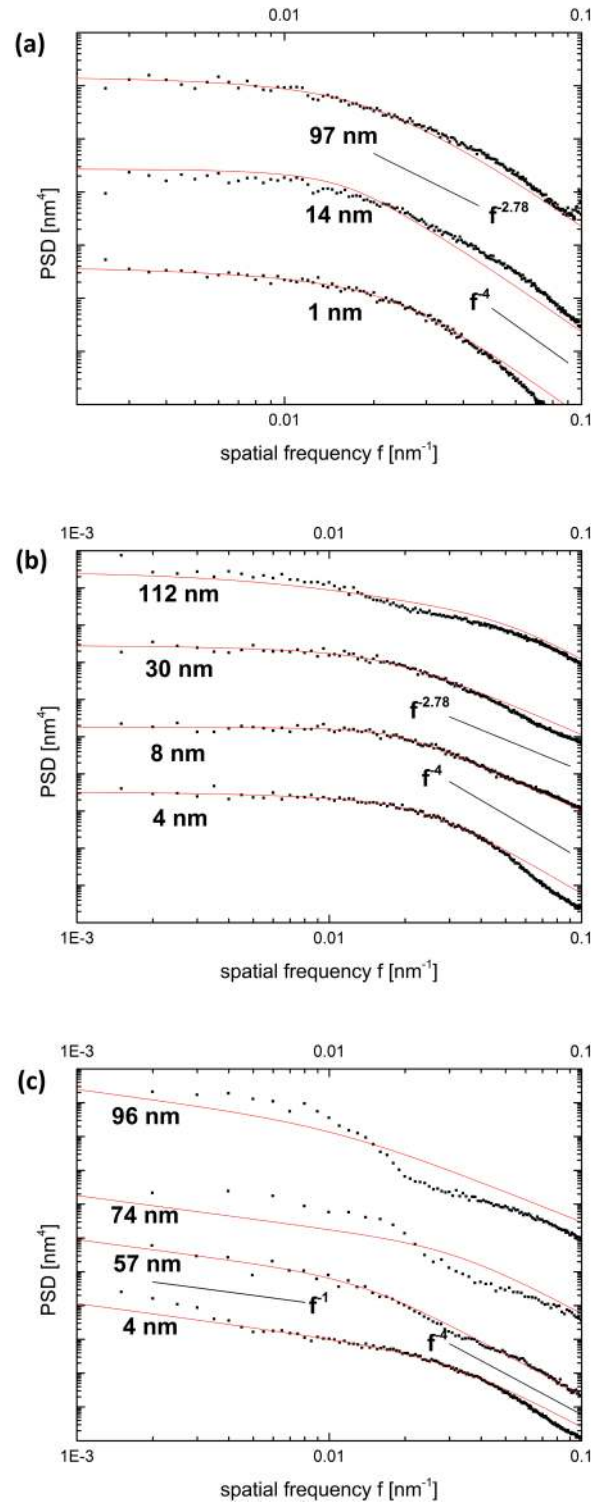

FIG. 4. The PSD function calculated from AFM measurements of Ge films with different thicknesses on various substrates: (a) amorphous films, deposited on Si at room temperature, (b) polycrystalline films, deposited on Si at 175 °C and (c) polycrystalline films, deposited on Ge at 175 °C.

thickness of 45 nm. It was calculated from the slope of the log-log representation of the roughness as a function of thickness. By fitting the roughness data, β=0.45±0.17 was obtained. Compared to the aforementioned growth exponents, random deposition gave the most adequate representation of this

roughening regime. Nevertheless, the values for growth dominated by diffusion and growth along the local surface were within the margins of error.

The roughening regime was analyzed by means of the height-height correlation function (see eq. 4). The separation of mounds was found by determining the distance of the first maximum to the center peak in the height-height correlation. After rescaling,[7] it could be shown, that the mound separation increased with the film thickness (see Fig. 2). The coarsening exponent was determined to be 0.48±0.29. This corresponded to a high coarsening rate, which was also found by Shin et al.[4] In that context, the high coarsening exponent was justified by defect-mediated filling of gaps and increased effective corner-diffusion, which was confirmed by the observation of irregularly shaped mounds (Fig. 1 (b)). The roughness evolution of Ge films deposited on Si substrates at room temperature and at 175 °C is depicted in Fig. 3. For small film thicknesses the RMS roughness increased slightly up to 0.2 nm corresponding to a polycrystalline film thickness of about 10 nm. After that, a smoothening regime occurred. For large film thicknesses (>50 nm) the roughness was rather constant.

For all films, only small differences between the roughness evolution of the amorphous and polycrystalline films were observed.

In Fig. 4, the evolution of the PSD function for different crystalline phases of the film and different substrate materials are presented. For the deposition of amorphous Ge on Si, the fits revealed that a_4 (see eq. 6) was large compared to the other constants, while a_3 was not negligible either. Mullins-Herring diffusion was therefore identified as the presumably dominating process. On small length scales, surface diffusion was important for the evolution of the surface. From the PSD curves at intermediate spatial frequencies ($f \approx 0.03$ nm^{-1}), the evolution of the topography could be described by the Kardar-Parisi-Zhang equation. This behavior was similar for all the film thicknesses shown here. For the deposition of polycrystalline Ge on Si, the fits revealed a comparably high a_4-constant for small film thickness (4 nm), while a_4=0 and a_3 dominated for medium film thickness (8 nm and 30 nm). In the beginning of the growth, surface diffusion as described by Mullins and Herring governed the process. After a certain film thickness, surface diffusion was suppressed and the quadratic term of the Kardar-Parisi-Zhang equation became more prominent. Traditionally the interpretation of this term has been desorption, however due to the relatively small deposition temperatures, desorption was assumed to be negligible here. Different, more complex mechanisms might also account for such a functional dependency. For high film thickness (112 nm), 'bumps' and irregularities in the PSD function appeared due to the formation of mound structures with characteristic separations.

For the deposition of polycrystalline Ge on Ge, the fits revealed domination of surface diffusion up to a film thickness of 57 nm. In these cases the PSD curves show an f^{-4}-behavior for large f and an f^{-1}-behavior for smaller f. Traditionally the f^{-1}-dependency has been interpreted as viscous flow.[21] It is to be noted however, that noise might have also contributed here. It is not possible to distinguish between noise and the real f^{-1}-dependency. For larger film thicknesses, again 'bumps' evolved, leading to relatively large deviations between the fits and measured data. The 'bumps' moved to lower spatial frequencies from film thicknesses of 74 nm to 96 nm. This shift indicated, that the average separation of mound-structures increased, as was also shown above by means of the height-height correlation.

Kinetic Monte-Carlo simulations of PLD of Si on Si have already been performed.[22] For thermal deposition, the occurrence of mound-like structures and existence of a second maximum in the height-height correlation were observed. Additionally the roughness exponent was determined to be $\alpha \approx 0.95 \pm 0.1$ for a deposition temperature of 400 °C. Comparable roughness exponents were found in this study at lower temperatures depending on the exact deposition conditions.

IV. SUMMARY

For the deposition of polycrystalline Ge on Ge at 175 °C the roughness of the films initially decreased. This regime was dominated by a Mullins-Herring diffusion process. Beginning at a certain film thickness (approx. 45 nm), a roughening occurred. This roughening was accompanied by the occurrence of mound-structures, which were observed in the height-height correlation function as well as in the PSD spectra. These changes were also accompanied by a comparably high coarsening rate.

For the deposition of amorphous Ge on Si at room temperature, the surfaces were smoothened after reaching film thicknesses of approx. 10 nm. Here, Mullins-Herring diffusion was found to be the governing mechanism on small length scales, independent of the film thickness. For the deposition of polycrystalline Ge at 175 °C, the surfaces were also smoothened after reaching film thicknesses of several nm. However, the Mullins-Herring diffusion was identified as present only for small film thickness (4 nm). For larger film thicknesses, surface diffusion was suppressed and the Kardar-Parisi-Zhang equation was a suitable description of the process already on small length scales.

ACKNOWLEDGMENTS

We would like to thank Dr. Erik Thelander for the technical assistance and for several useful discussions and Emilia Wisotzki for proofreading the manuscript.

[1] H. M. Smith and A. F. Turner, Appl. Optics **4**, 147 (1965).
[2] P. R. Willmott and J. R. Huber, Rev. Mod. Phys. **72**, 315 (2000).
[3] M. Stafe, A. Marcu, and N. Puscas, *Pulsed Laser Ablation of Solids*, Springer Series in Surface Sciences 53, Springer, 2014.
[4] B. Shin, J. P. Leonard, J. W. McCamy, and M. J. Aziz, Appl. Phys. Lett. **87**, 181916 (2005).
[5] M. J. Aziz, Appl. Phys. A **93**, 579 (2008).
[6] B. Shin and M. J. Aziz, Phys. Rev. B **76**, 085431 (2008).
[7] C. V. Cojocaru, A. Bernardi, J. S. Reparaz, M. I. Alonso, J. M. MacLeod, C. Harnagea, and F. Rosei, Appl. Phys. Lett. **91**, 113112 (2007).
[8] P.-O. Jubert, O. Fruchart, and C. Meyer, Surf. Sci. **522**, 8 (2003).
[9] J. Röder, T. Liese, and H.-U. Krebs, J. Appl. Phys. **107**, 103515 (2010).
[10] S. G. Mayr and R. S. Averback, Phys. Rev. Lett. **87**, 196106 (2001).
[11] J. T. Drotar, Y.-P. Zhao, T.-M. Lu, and G.-C. Wang, Phys. Rev. B **62**, 2118 (2000).
[12] D. E. Wolf and J. Villain, Europhys. Lett. **13**, 389 (1990).
[13] W. Mullins, J. Appl. Phys. **28**, 333 (1957).
[14] C. Herring, J. Appl. Phys. **21**, 301 (1950).
[15] A. L. Barabasi and H. E. Stanley, *Fractal Concepts of Surface Growth* (Cambridge University Press, 1995).
[16] M. Kardar, G. Parisi, and Y. C. Zhang, Phys. Rev. Lett. **56**, 889 (1986).
[17] J. G. Amar and F. Family, Phys. Rev. A **41**, 3399 (1990).
[18] W. M. Tong and R. S. Williams, Annu. Rev. Phys. Chem. **45**, 401 (1994).
[19] Y. Zhao, G.-C. Wang, and T.-M. Lu, *Characterization of amorphous and Crystalline Rough Surfaces: Principles and Applications* (Academic Press, San Diego, 2001).
[20] A. N. Larsen, Mat. Sci. Semicon. Proc. **9**, 454 (2006).
[21] C. C. Umbach, R. H. Headrick, and K.-C. Chang, Phys. Rev. Lett. **87**, 246104 (2001).
[22] S. G. Mayr, M. Moske, K. Samwer, M. E. Taylor, and H. A. Atwater, Appl. Phys. Lett. **75**, 4091 (1999).